

Time dependence of isotopic temperatures

Armando Barrañón^a, Claudio O. Dorso^b, Jorge A. López^{c,*}

^a *Universidad Autónoma Metropolitana–Azcapotzalco, México D.F., Mexico*

^b *Universidad de Buenos Aires, Nuñez, Argentina*

^c *University of Texas at El Paso, El Paso, TX 79968, USA*

Received 4 October 2006; received in revised form 22 March 2007; accepted 12 April 2007

Available online 20 April 2007

This work is dedicated to the memory of Vijay R. Pandharipande

Abstract

In this study the double isotope yield ratio thermometer, commonly used in heavy ion reactions, is put to the test in molecular dynamics simulations for a variety of nuclear reactions and energies. Comparing results to other estimates of the temperature and to experimental measurements, it is determined that the double isotope yield temperature indeed reflects the hot and dense phase of the reaction. Correlations between the double isotope yield temperature, the system size, beam energies, and collision times were investigated.

© 2007 Elsevier B.V. All rights reserved.

Keywords: Heavy ion collisions; Nuclear fragmentation

1. Introduction

A precise determination of the temperature achieved in nuclear reactions has become a priority in the study of heavy ion reactions. For example, recent investigations involving radioactive isotopes [1–5] promise to elucidate the role of the asymmetry mass terms of the nuclear equation of state through the phenomenon of isoscaling. For this, however, similar but isotopically different reactions must reach a common equilibrium temperature T at the same time. As the resolution needed to determine this *thermal symmetry* between different reactions is very high, a study of the time evolution of the reaction's temperature is clearly in order.

* Corresponding author.

E-mail address: jorgelopez@utep.edu (J.A. López).

A recent study of such time dependence was performed using the kinetic energy variation of emitted light clusters [6]. Based on results from theoretical models [7,8] and experiments [9,10] that show a correlation between the emission time and the energy of early emitted particles, the study uses the *AMD-V* model [8] to calibrate the emission time scales and follow the time evolution of the system. Although this analysis illuminates interesting features of the kinetics of the reaction, we believe it has to be confirmed by an independent approach.

Thus the motivation of the present study: to understand what one of the most commonly used indicators of temperature, the double isotope yield ratio thermometer, measures in a heavy ion reaction. This will be done using a molecular dynamics code, *Latino*, which will simulate the experimental reactions using the same combination of nuclei and beam energies as the experimental study.

The structure of the article is as follows: in the next section the different measures of the temperature to be used will be briefly introduced and connected to molecular dynamics. Then, these measures will be used in Section 3 in two different situations: to a study case, in Section 3.1, in which the production of the different species is carefully dissected for the full understanding of the thermometers; and, in Section 3.2, to a variety of reactions and beam energies for comparison to experimental data. The paper will close with some conclusions in Section 4.

2. Measuring temperature in heavy ion reactions

As the temperature of a nuclear reaction cannot be uniquely defined, it is best to describe the reaction with a plausible scenario. Basic arguments [11,12] suggest that collisions can fuse the participating nuclei, initially at normal density, zero temperature, and zero entropy, into a compound nucleus that reaches a maximum density, temperature and entropy, which then bounces into an expansion that drives the system into the fragmentation [13,14]. Under this scenario, it is clear that temperature can only be defined in a conditional manner.

2.1. Measuring the temperature in molecular dynamics

As heavy ion reactions take nuclei from equilibrium to a hot and dense phase, and then to an expanding and disassembling state, its study requires a model capable of reproducing the collision dynamics including stages in- and out-of-thermal equilibrium. As statistical and other equilibrium and dynamical models [15–21] lack—by construction—of all relevant collision-induced correlations or of all higher-order correlations needed to produce appropriate fragmentation, in this study we use a molecular dynamics (MD) model that can describe non-equilibrium dynamics and changes of phase without adjustable parameters.

The model “*Latino*” [22], which uses the Pandharipande potential (Coulomb plus a two-body nuclear [23]) and a fragment-recognition algorithm [24], reproduces nucleon–nucleon cross sections, the correct binding energies and densities of real nuclei. In the recent past it has been used to study neck fragmentation [13], phase transitions [25], critical phenomena [26,27], the caloric curve [14,28], and—most recently—isoscaling [29] in nuclear reactions.

With this model one can obtain an approximate view of the thermalization process [30]. After the biggest fragment is identified during a collision (through *ECRA* [24], *MSTE* or another method), its temperature can be calculated from the nucleon’s kinetic energies $\{K_i\}$ (with respect to the center of mass of the moving fragment) through $T_{BF} = \sum_i 2K_i/3N$. Tracking the fragment during the collision can help us determine T_{BF} as a function of time.

To avoid puristic discussions on whether such an evolving measure over a small system would correspond to a *real* temperature, one could instead determine temperature-like dynamical quantities to demonstrate thermalization and other features [29], or one could talk instead about single-time measures such as the *breakup* or *transition* temperature [14] (i.e., the temperature at which the system ruptures); these measures, however, yield in practice a picture consistent with T_{BF} .

2.2. Temperature from the double isotope yield ratio

On the other hand, as the time evolution of T_{BF} cannot be determined directly from experimental observations, nuclear experimentalists must resort to particle-emitting processes to infer the temperature of a reaction. Options favored by experimentalists are the thermometers based on particle yields, from excited population of certain species, and from ratios of particles yields (for applications see e.g. [31–33]). In this study we take advantage of the fully detailed microscopic view that *Latino* provides us with, to understand the meaning of one of this measures, the temperature from the double isotope yield ratio.

The yield ratios of two adjacent isotopes of two different elements allows to obtain the temperature of an emitting compound system at chemical and thermal equilibrium [33]. This thermometer has been used to determine the caloric curve and other features of fragmentation experiments [32,34–38]. Following [6,39], the temperature T_{HHe} of a source can be estimated from the yields of d, t, ^3He and ^4He through

$$T_{\text{HHe}} = \frac{14.3}{\ln[1.59(9/8)^{1/2} \frac{Y_t/Y_d}{Y_{^4\text{He}}/Y_{^3\text{He}}}] } \quad (1)$$

where Y_t , Y_d , $Y_{^4\text{He}}$ and $Y_{^3\text{He}}$ are the yields of such species. As it will be obvious below, choosing abundant species, such as d, t, ^3He and ^4He , helps to obtain statistics robust enough as to be able to compute their yields as a function of time, and to track the evolution of T_{HHe} during the reaction. To avoid the contamination of this temperature by *non-thermal* emission, any estimation of T_{HHe} must exclude the so-called promptly emitted particles (PEPs) which are emitted in the initial contact of the colliding nuclei.

Even though expression (1) was obtained using quantum statistical thermodynamical arguments, a similar relationship can be expected for classical systems. Using Fisher's droplet formula, $Y(A_1) \propto A_1^{-\tau} e^{(a_0\omega\epsilon T_c A_1^\sigma)/kT} e^{((\mu-\mu_c)/kT)A_1}$, where A_1 is the mass of the fragment, ϵ is the distance to the critical point, ω is the surface entropy density, μ is the chemical potential, μ_c is the value at coexistence, and σ , τ are the critical exponents, the double ratio of numbers of fragments for species differing in one constituent is given by

$$R = \frac{Y(A_1)Y(A_2+1)}{Y(A_1+1)Y(A_2)} = \left[\frac{A_1(A_2+1)}{(A_1+1)A_2} \right]^{-\tau} e^{(a_0\epsilon T_c(\omega A_1^\sigma - \omega(A_1+1)^\sigma - \omega A_2 + \omega(A_2+1))/kT)},$$

which has the same shape as the expression found in [39]. From this

$$\log R = -\tau \log \left[\frac{A_1(A_2+1)}{(A_1+1)A_2} \right] + \frac{1}{kT} \alpha [\omega A_1^\sigma - \omega(A_1+1)^\sigma - \omega A_2^\sigma + \omega(A_2+1)^\sigma]$$

with $\alpha = a_0\epsilon T_c$, and, under the assumption of uniform ω , we thus obtain an expression similar to Albergo's:

$$kT = \frac{C}{\log \left[\frac{Y(A_1)Y(A_2+1)}{Y(A_1+1)Y(A_2)} \right] Q}$$

where

$$\mathbb{C} = \alpha\omega[A_1^\sigma - (A_1 + 1)^\sigma - A_2^\sigma + (A_2 + 1)^\sigma], \quad \mathbb{Q} = [A_1(A_2 + 1)/(A_1 + 1)A_2]^\tau.$$

In spite of having an expression valid for classical systems, for the sake of comparison to other estimates, in the present work we continue using expression (1) with the coefficients obtained for a Fermi gas of nucleons. The extension of such a model to the present case of a classical model should not present any problems as the Fermi–Dirac and Boltzmann statistics converge when the de Broglie wavelength, $\Lambda^3 = (h^2/2\pi mT)^{3/2}$, is comparable to the nuclear volume [40], as it is the case in the hot and dense phase of the reaction.

3. Time evolution of temperature

3.1. A case study: $^{40}\text{Ca} + ^{40}\text{Ca}$ at 35 MeV/A

Two hundred simulations of central collisions were performed for the reaction $^{40}\text{Ca} + ^{40}\text{Ca}$ at a beam energy of $E = 35$ MeV/A. For each collision—and for several times during each collision—the biggest fragment was identified through the *MSTE* method [24], and its temperature T_{BF} was calculated as described in Section 2. Likewise, the production of d, t, ^3He and ^4He was tracked as a function of time, and the T_{HHe} was obtained from it through (1) both from the *instantaneous* yields (i.e., those produced in intervals of 5 fm/c), as well as from the accumulated ones.

Fig. 1 shows the time evolution of the particle yields and the temperatures obtained for these collisions. The top panel shows the evolution of the yield of d, t, ^3He and ^4He (in arbitrary units) contrasted with the size of the biggest fragment (in mass number). The bottom panel shows the T_{HHe} obtained from the instantaneous yields (dots) contrasted with T_{BF} , the kinetic temperature of the largest fragment (dashed line), and with the T_{HHe} of the accumulated yields (solid line).

Several observations are immediate. The production of d, t, ^3He and ^4He starts while the colliding nuclei are still merged into a single blob of 80 nucleons. There is no noticeable simultaneous production of the four species while the biggest fragment is at its maximum temperature; as the instantaneous production reaches its maximum, the biggest fragment cools and reduces its size considerably.

The temperature obtained from the instantaneous yields has three distinct regions: an initial one with a large primary spike (out of scale), a second one composed of a smooth peak and a long decaying plateau, and a final one in which T_{HHe} becomes alive again with a series of smaller peaks.

The smooth long-tailed peak that follows the spike, is produced when the particle production is at its maximum (cf. top panel) and, thus, when the statistics are more reliable. Judging from the shrinking size of the biggest fragment at that time, that abundant production of light particles originates from this fragment; this confirms T_{HHe} as *bona fide* thermometer of this stage of the reaction. Furthermore, the general behavior of this long-tailed peak is reminiscent of that observed in experimental data [6].

The later peaks of T_{HHe} , which appear after 100 fm/c, correspond to the end tail of the particle production. In this stage the size of the biggest fragment has stabilized and is finishing evaporating. Again, due to shrinking statistics, these peaks cannot be taken as reliable indicators of the system's temperature.

The fact that the production of light particles during the period of maximum evaporation (i.e., from 50 to 100 fm/c) overwhelms the rest, makes the T_{HHe} obtained from the cumulative

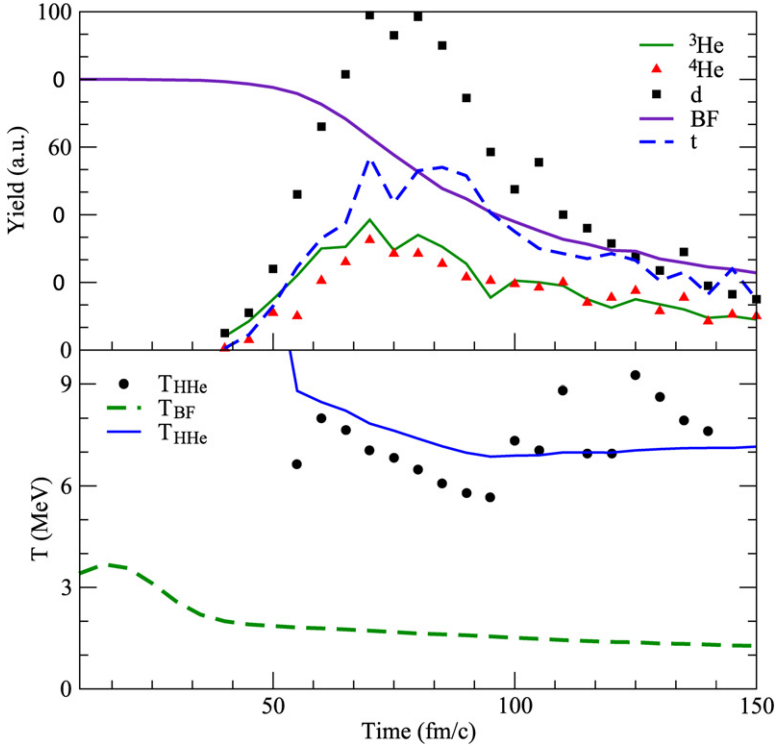


Fig. 1. Time evolution of yields and temperatures obtained from 200 central collisions of ${}^{40}\text{Ca} + {}^{40}\text{Ca}$ at 35 MeV/A; The top panel shows the yields compared to the size of the biggest fragment. The bottom panel shows the T_{HHe} obtained from the instantaneous yields (dots), T_{BF} (dashed line), and T_{HHe} from the accumulated yields (solid line).

production (solid line in the bottom panel) give a steady value consistent with the instantaneous T_{HHe} of the smooth long-tailed peak. This finding is bound to simplify the calculation of T_{HHe} from experimental data, as a good estimate of it can be obtained from the total particle production without having to filter out later decays.

Although in this case study T_{HHe} appeared larger in magnitude than T_{BF} , this is not a general result, as it will be seen next.

3.2. Energy and mass dependence of T_{HHe}

Repeating the previous exercise for reactions at different energies and with different ions helps us understand the dependence of T_{HHe} on beam energy and total mass. Two hundred central collisions were performed for each of the reactions ${}^{64}\text{Zn} + {}^{58}\text{Ni}$, ${}^{64}\text{Zn} + {}^{92}\text{Mo}$ and ${}^{64}\text{Zn} + {}^{197}\text{Au}$ at beam energies of $E = 25, 35$ and 47 MeV/A; Figs. 2, 3, and 4 present the time evolution of the corresponding temperatures.

Figs. 2, 3, and 4 show the behavior of T_{HHe} , now obtained from the cumulative production of light particles, and contrasted with T_{BF} . To get a more realistic count, comparable to that of experiments, this time all emissions of d , t , ${}^3\text{He}$ and ${}^4\text{He}$ were counted regardless of whether they were produced by the biggest fragment or not.

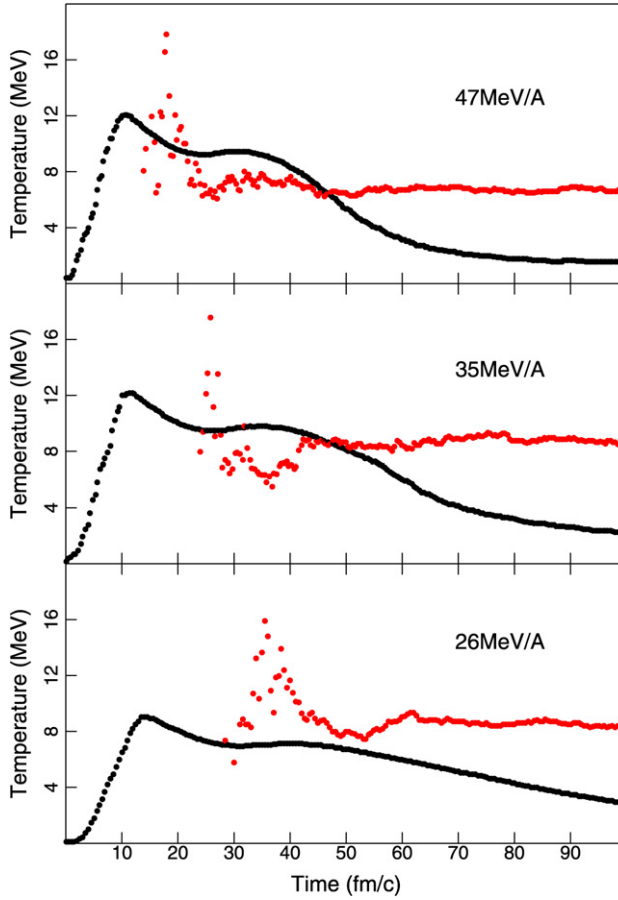


Fig. 2. Time evolution of T_{BF} , the temperature of the biggest fragment, and of T_{HHe} obtained from the cumulative production of light particles of central collisions of $^{64}\text{Zn} + ^{58}\text{Ni}$ at beam energies of $E = 25, 35$ and 47 MeV/A. T_{BF} starts from zero time while T_{HHe} does not get established until later in the reaction.

Once more, several observations are immediate. The general shape of T_{HHe} appears as before, a long-tailed peak with the maximum much more pronounced and of magnitude comparable to T_{BF} . Due to the use of the accumulated yields, T_{HHe} no longer presents the late-time oscillations observed in the instantaneous temperature, and instead it shows a very steady asymptotic value.

Again, the fact that T_{HHe} achieves a sizeable value while T_{BF} has decreased into a plateau from its maximum, can be taken as an indication that the light particles responsible for T_{HHe} were produced from evaporation of an equilibrated source.

Although no direct correlation is obvious between the peaks of T_{HHe} and the system size or beam energies, an increasing trend is observed between the peak and the plateau values of T_{BF} and the system size. On the other hand, the asymptotic value of the cumulative T_{HHe} shows little dependence on the system size or collision energy.

Table 1 summarizes the size and energy variation of the peak values of T_{BF} and T_{HHe} of Figs. 2, 3, and 4, and compares them to the peak temperatures obtained experimentally (as de-

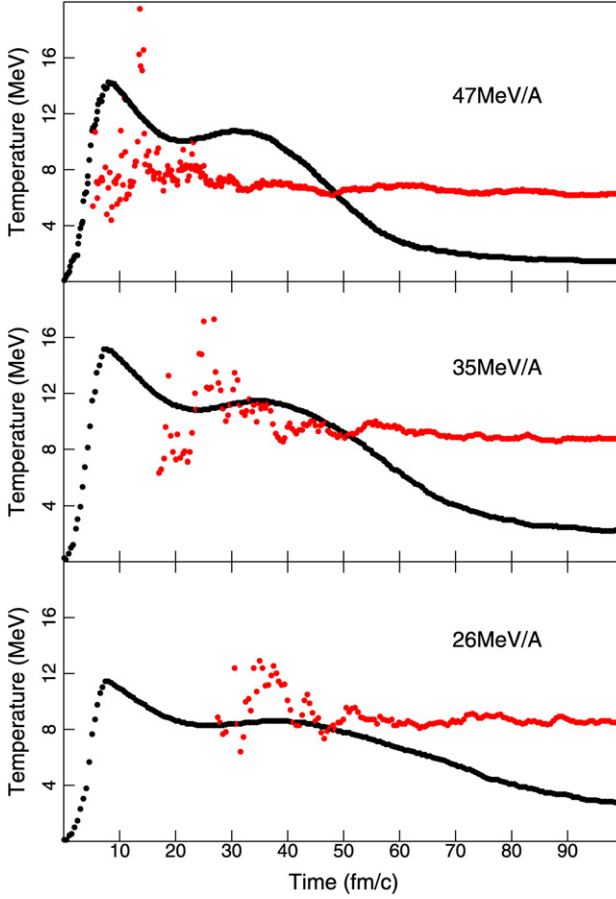


Fig. 3. Same as previous figure for $^{64}\text{Zn} + ^{92}\text{Mo}$.

Table 1
Peak temperatures

Reaction	Energy	T_{BF}	T_{HHe}	Experimental
$^{64}\text{Zn} + ^{58}\text{Ni}$	26	6.8	11.9	9.5
	35	9.1	13.2	16.5
	47	12	17.8	25
$^{64}\text{Zn} + ^{92}\text{Mo}$	26	8.6	9.7	11
	35	11.4	12.7	13
	47	14.2	19.5	17.5
$^{64}\text{Zn} + ^{197}\text{Au}$	26	10.6	13.8	10
	35	12.8	13.6	12
	47	14.44	13.9	15.5

terminated by inspection from the published literature [6]). The experimental peaks appear to have similar values as the peaks of T_{HHe} obtained from the MD calculations.

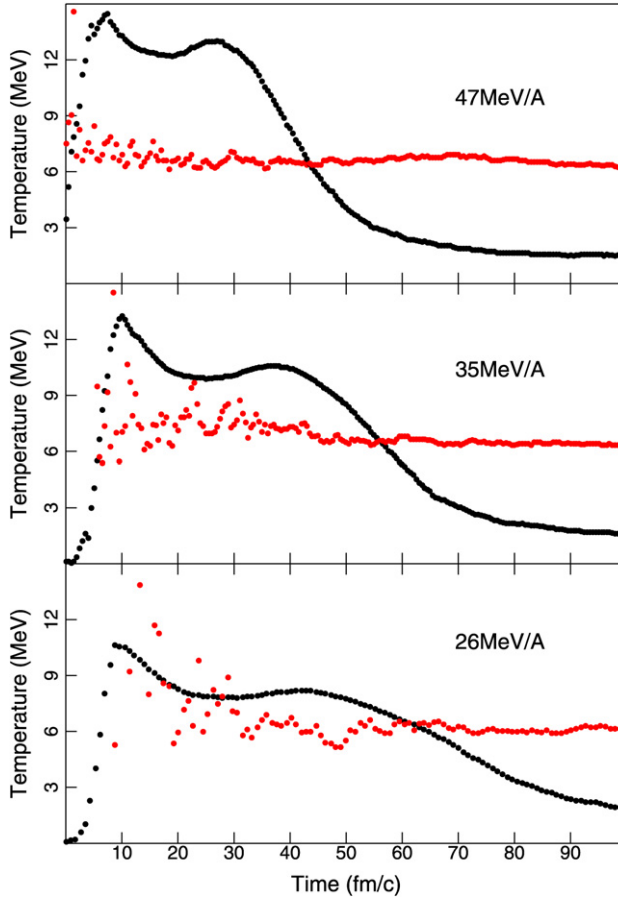


Fig. 4. Same as previous figure for $^{64}\text{Zn} + ^{197}\text{Au}$.

Further comparison with the experimental results shows discrepancies in the time scale of the temperature. While in our model the peaks of T_{HHe} are produced before, say, 50 fm/c for all reactions and energies, experimental results show peaks in the 100 to 150 fm/c. As the MD code used in the present work does not have any adjustable parameters, we attribute this difference to the model-dependent method used in reference [6] to estimate the times. Indeed *AMD-V* reports a starting time for light particle emission of 50 fm/c, time at which *Latino* has stabilized its light particle emission. Another probable origin for this time difference is a possible mixing of particles from different sources (projectile, participant and spectator) as indicated by the experimentalists.

4. Conclusions

In this study we performed a study of the double isotope yield ratio temperature achieved in heavy ion reactions. We did this by first showing that the temperature of systems obeying Fisher's law, such as ours, can be determined through a double isotope yield much like in the Fermi gas case, i.e., in Albergo's case. Second, molecular dynamics simulations were used for a variety

of reactions and energies, to extract the temperature T_{HHe} and compared it both to the kinetic temperature of the largest fragment and to experimental measurements.

The time evolution of the temperature T_{HHe} was obtained using the instantaneous and cumulative yields of the isotopes d, t, ^3He , and ^4He .

The instantaneous yields of these isotopes were found to increase substantially during the hot and dense phase of the reaction, confirming the reliability of T_{HHe} as an indicator of the thermal conditions of the reaction.

The cumulative temperature, obtained with the time-integrated yields, presented a correlation with the temperature of the biggest fragment, T_{BF} ; this relationship, however, cannot be firmly elucidated from this study as T_{HHe} was obtained using the parameters for a Fermi gas. Additionally, T_{HHe} appears to be correlated with the reaction's beam energies and, in all studied cases, its asymptotic value tended to ≈ 6 MeV.

Although the scale of values of the cumulative T_{HHe} (and its maximum peak value) agrees nicely to experimental data, other features of the T_{HHe} peaks, such as shape and timing, are different than those obtained by the experimentalists; this could be due to the model-dependent method used to estimate the timing and—thus—the shape of the temperature curves.

Several points of T_{HHe} remain to be further explored: the asymptotic value of the cumulative temperature, its dependence on beam energy and mass, its connection to the kinetic temperature, etc.; these and other topics are currently being studied and will be reported shortly.

Acknowledgements

A.B., J.A.L. and C.O.D. thank the University of Colima and the University of Texas at El Paso, respectively, for their hospitality while part of this work was carried out. The authors are indebted to C.R. Escudero for his help with Fig. 1.

References

- [1] H.S. Xu, M.B. Tsang, T.X. Liu, X.D. Liu, W.G. Lynch, W.P. Tan, A. Vander Molen, G. Verde, A. Wagner, H.F. Xi, C.K. Gelbke, L. Beaulieu, B. Davin, Y. Larochele, T. Lefort, R.T. de Souza, R. Yanez, V.E. Viola, R.J. Charity, L.G. Sobotka, Phys. Rev. Lett. 85 (2000) 716.
- [2] H. Johnston, et al., Phys. Lett. B 3715 (1996) 186.
- [3] R. Laforest, et al., Phys. Lett. C 59 (1999) 2567.
- [4] M.B. Tsang, C.K. Gelbke, X.D. Liu, W.G. Lynch, W.P. Tan, G. Verde, H.S. Xu, W.A. Friedman, R. Donangelo, S.R. Souza, C.B. Das, S. Das Gupta, D. Zhabinsky, Study of isoscaling with statistical multifragmentation models, Phys. Rev. C 64 (2002) 054615.
- [5] M.B. Tsang, W.A. Friedman, C.K. Gelbke, W.G. Lynch, G. Verde, H. Xu, Phys. Rev. Lett. 86 (2001) 5023.
- [6] J. Wang, et al., Phys. Rev. C 72 (2005) 024603.
- [7] J. Lukasik, et al., Acta Phys. Pol. B 24 (1993) 1959.
- [8] A. Ono, H. Horiuchi, Phys. Rev. C 53 (1996) 2958.
- [9] Z.Y. He, et al., Phys. Rev. C 57 (1998) 1824.
- [10] C.J. Gelderloset, et al., Phys. Rev. C 52 (1995) R2834.
- [11] G.F. Bertsch, P. Siemens, Phys. Lett. B 126 (1983) 9.
- [12] J.A. López, P. Siemens, Nucl. Phys. A 314 (1984) 465.
- [13] A. Chernomoretz, L. Gingras, Y. Larochele, L. Beaulieu, R. Roy, C. St-Pierre, C.O. Dorso, Phys. Rev. C 65 (2002) 054613.
- [14] A. Barrañón, J. Escamilla, J.A. López, Phys. Rev. C 69 (2004) 014601.
- [15] J.P. Bondorf, A.S. Botvina, A.S. Iljinov, L.N. Mishustin, K. Sneppen, Phys. Rep. 257 (1995) 133.
- [16] W.A. Friedman, Phys. Rev. Lett. 60 (1988) 2125;
W.A. Friedman, Phys. Rev. C 42 (1990) 667.
- [17] G.F. Bertsch, S. Das Gupta, Phys. Rep. 160 (1988) 190.

- [18] P. Danielewicz, Nucl. Phys. A 673 (2000) 375.
- [19] B.-A. Li, Phys. Rev. Lett. 85 (2000) 4221.
- [20] J. Aichelin, H. Stöcker, Phys. Lett. B 176 (1986) 14.
- [21] A. Ono, P. Danielewicz, W.A. Friedman, W.G. Lynch, M.B. Tsang, Phys. Rev. C 68 (2003) 051601.
- [22] A. Barrañón, A. Chermomoretz, C.O. Dorso, J.A. López, J. Morales, Rev. Mex. Fís. 45 (Suppl. 2) (1999) 110.
- [23] R.J. Lenk, T.J. Schlagel, V.R. Pandharipande, Phys. Rev. C 42 (1990) 372.
- [24] A. Strachan, C.O. Dorso, Phys. Rev. C 56 (1997) 995.
- [25] A. Barrañón, C.O. Dorso, J.A. López, Rev. Mex. Fís. 47 (Suppl. 2) (2001) 93.
- [26] A. Barrañón, R. Cárdenas, C.O. Dorso, J.A. López, Heavy Ion Phys. 17 (1) (2003) 59.
- [27] A. Barrañón, C.O. Dorso, J.A. López, Inf. Technol. 14 (2003) 31.
- [28] A. Barrañón, J. Escamilla, J.A. López, Braz. J. Phys. 34 (2004) 904.
- [29] C. Dorso, C.R. Escudero, M. Ison, J. López, Phys. Rev. C 73 (2006) 044601.
- [30] M.J. Ison, C.O. Dorso, Phys. Rev. C 71 (2005) 064603.
- [31] T. Odeh, et al., Phys. Rev. Lett. 84 (2000) 4557.
- [32] W. Bauer, Phys. Rev. C 51 (1995) 803.
- [33] S. Albergo, S. Costa, E. Costanzo, A. Rubbino, Nuovo Cimento A 89 (1985) 1.
- [34] J. Pochodzalla, et al., Phys. Rev. Lett. 75 (1995) 1040.
- [35] J. Pochodzalla, et al., Phys. Rev. C 35 (1987) 1695.
- [36] V. Serfling, et al., Phys. Rev. Lett. 80 (1998) 3928.
- [37] H. Xi, et al., Z. Phys. A (1997) 397.
- [38] J.B. Natowitz, et al., Phys. Rev. C 65 (2002) 034618.
- [39] A. Kolomiets, V.M. Kolomietz, S. Shlomo, Phys. Rev. C 55 (1996) 1376.
- [40] J.A. López, C.O. Dorso, Lecture Notes on Phase Transitions in Nuclear Matter, World Scientific, ISBN 981-02-4007-4, 2000.